Assessment of metal immission in urban environments using elemental concentrations and Zn isotope signatures in leaves of *Nerium oleander*

Martín, A.[1, 2], Caldelas, C.[3], Weiss, D.[4], Aranjuelo, I.[5] and Navarro, E.[1*]

[1] Pyrenean Institute of Ecology-CSIC. Avda. Montañana, 1005. 50.059 Zaragoza,Spain.

[2] San Jorge University. Campus Universitario Villanueva de Gállego. Autovía A-23 Zaragoza-Huesca Km. 299, 50.830 Villanueva de Gállego (Zaragoza), Spain.

[3]Department of Evolutionary Biology, Ecology and Environmental Sciences, University of Barcelona, Avda. Diagonal, 643, 08028 Barcelona, Spain.

[4]Department of Earth Science and Engineering, Imperial College of London, London SW7 2AZ, UK.

[5] Agrobiotechnology Institute (IdAB)-CSIC-UPNA-GN, Avenida Pamplona 123, Mutilva Baja (Navarra), Spain.

* Corresponding author: enrique.navarro@ipe.csic.es

ABSTRACT

A thorough knowledge of spatial and temporal emission and immission patterns of air pollutants in urban areas is often limited because of the low number of air-quality monitoring stations available. Plants are promising low-cost biomonitoring tools. However, source identification of the trace metals incorporated in plant tissues (i.e. natural vs. anthropogenic) and the identification of the best plant to use remain fundamental challenges. To this end, *Nerium oleander* L. collected in the city of Zaragoza (NE Spain) has been investigated as a biomonitoring tool for assessing the spatial immission patterns of airborne metals (Pb, Cu, Cr, Ni, Ce, and Zn). *N. oleander* leaves were sampled at 118 locations across the city, including the city center, industrial hotspots, ring-roads, and outskirts. Metal concentrations were generally higher within a 4 km radius around the city center. Calculated enrichment factors relative to upper continental crust suggested an anthropogenic origin for most of them. Zinc isotopes showed a significant variability that may be linked to different pollution sources. Plants closer to industrial hotspots and the city centre had the heaviest Zn isotopic compositions (δZn_{Lyon} up to 0.70‰), while those far away were isotopically light (up to -0.85‰). This information may be applied for improving the environmental and human risk assessment related to the exposure to air pollution in urban areas.

Keywords: Zinc stable isotopes, air pollution, biomonitoring, trace element, galvanization, pollution tracing, aerosols, aluminum, copper, nickel, lead

1. INTRODUCTION

More than 70% of the European population live in urban areas, often exposed to elevated levels of air pollutants. These are emitted from a variety of urban sources; the most important

of these are road traffic, domestic dwellings, industrial facilities, and power generation plants [1]. Traditional air pollutants include sulphur dioxide (SO_2), nitrogen oxides (NO_x), carbon monoxide (CO), lead (Pb), particulate matter (PM), ozone (O_3), and volatile organic compounds (VOCs). Nowadays a new category of Hazardous air pollutants (HAPs) is rising concern for its potential impacts on human health: metals, mineral fibres (i.e. asbestos), gases, polycyclic aromatic hydrocarbons (PAHs), dioxins, and others. Industrial activity, traffic, urbanization, and agricultural activities have been identified as target sources of environmental pollution. HAPs such as metals are not biodegradable and tend to accumulate in living organisms and many metal ions are known to be toxic or carcinogenic. While some metals (such as zinc, iron, and copper), are considered essential for plants and animals, above certain concentration values they can be very toxic and cause adverse effects in human health [2]. The respiratory and cardio-vascular systems have been described to be strongly compromised by elevated levels of particulate matter, resulting in increased morbidity and mortality rates in urban areas. Monitoring efforts generally concentrate on the "traditional" pollutants, while HAPs are often only measured on a spatially and temporally restricted scale in monitoring programs [1]. So, even if the European Environment Agency recommends: "to present and map air quality in Europe at relevant spatial and temporal scales" and "to provide quantitative relationships between air quality and the source emissions responsible" [1], most EU cities have not yet implemented monitoring programs addressing such recommendations.

One particular aspect of concern in urban air pollution is particulate matter (PM) [3]. The long residence time of fine PM facilitates the dispersal over large areas away from their emission sources [4]. The emission of Pb, Cu, Cd, Ni, and Zn has been increasing in the urban environments due to rising industrial production (waste incineration, power plants, metal refining, galvanization, etc…), traffic intensification (tires, exhaust particles, brake discs, and others), and increased runoff from road furniture (road signals, paints) [5]. Such PM might be either dispersed by the wind or precipitate in rainfall with the consequent contamination of soil and water. Immission patterns based on road traffic density assessments are often unusable because of the limited number of air-quality monitoring stations available in cities. However, a detailed understanding of the immission pattern is a requisite for developing targeted policies to prevent human and environmental exposure to such pollutants.

Knowledge on local and regional distribution of airborne particle-bound substances and their toxic, genotoxic, and ecotoxic potential is still very limited. Furthermore, atmospheric pollutant content analyses cannot be always directly linked to potential adverse effects on human beings, because the sensitivity to air pollution is influenced by many abiotic and biotic factors not considered in such determinations [6]. For this reason, biomonitoring of ambient pollution using bioindicator plants has been suggested by European authorities (i.e. ''Directive relating to arsenic, cadmium, mercury, nickel, and PAHs in ambient air'', EU 2004). Bioindicator plants proportionate valuable information of the spatial and temporal distribution of air pollutants. Moreover, the use of plants is well established [7] and it is generally less expensive than conventional methods of air sampling (i.e. based on automated stations). That allows for more detailed spatial and temporal studies of pollutants immission [8] and for the identification of emission sources and the verification of the dispersion routes of pollutants [9, 10].

Pollutant absorption by plants takes place through roots and leaf stomata [11] depending on the form where the pollutants are available in the media. When pollutants are present in soil or water, they are taken up together with other essential and non-essential elements in response to concentration gradients induced by the selective uptake of ions by roots, or by element diffusion in the soil. Plants have evolved specific mechanisms to absorb nutrients from soil, and transport them from roots to shoots by radial transportation and xylem loading. While pollutant absorption by the roots has been most frequently described in the bibliography, stomatal opening has also been observed to be an important entrance of air pollutants within the leaves [12]. Moreover, stomatal responsiveness to air pollutants has been described as a complex process conditioned by pollutant concentration, the environmental conditions, the plant's age, and the species [13]. In fact, stomatal density and opening have been described to increase at low pollutant concentrations [12]; inversely both factors show a marked decrease in highly polluted environments, to reduce the exposure to pollution [14].

Nerium oleander L is a preferred plant for several reasons: (i) This species is widely distributed in urban areas as ornamental or barrier plant and it is perennial; (ii) sampling, identification and cultivation is easy and inexpensive, and (iii) it is resistant to pollution and droughts. This species has been used in studies of atmospheric pollution in various cities in Europe [8, 9, 15-20], showing a good capacity for bioaccumulating different metals as Pb, Cr, Cu, Li, Ni, and Zn [15]. However source identification of the trace metals incorporated in plant tissues (i.e. natural vs. anthropogenic) remains a fundamental challenge in immission studies.

Stable isotope ratios can provide important insight with respect to the sources of pollutants. This has been demonstrated with great success for lead, which has been widely used in lichens and other bio-monitors to identify gasoline-derived sources [21]. Since geological and industrial processes modify the isotopic ratios[22], these can be used for tracing the origin of the metals. Elevated Zn content combined with specific Zn isotopic signatures ($\delta^{66}Zn$) reported in lichens from periurban regions, point to the traffic as a source for such metal [23]. This isotope system has been also measured in lichens around a mining facility, with Zn signatures heavier (presenting signature of the ore body mined) than that of the natural dust originated from the local host rocks [24]. In other study, Zn isotopic signature allowed for identifying the industrial sources of pollution (a mining and smelting site) affecting peat surface layers [25], or for identifying different urban sources [26].

According to different air quality guidelines (US Environmental Protection Agency, World Health Organization or that of European Commission) Zaragoza is classed as a moderately polluted city [27], and Zn the metal with highest concentrations, i.e. a mean value of 212 ng m^{-3} [27]. The air quality of Zaragoza is influenced by the main industrial valley located in the north east, where various metal processing industries are located (metallurgical factories and alloy and galvanizing industries). Accordingly, the last report published by the local government, suggested that most of the Zn emitted to the atmosphere would come from these industrial activities, although road traffic was also suggested as a potentially relevant contributor [28].

Therefore, the working hypothesis of this study is that the differences in Zn isotopic signatures between samples and their spatial distribution will allow for a screening of the different pollution emission sources in the urban area. Accordingly leaves of *N. oleander* were sampled across the city and their metal content and Zn isotopic signature were characterized. Special

attention was paid to the traffic density and the location of metal-related industries as potential sources for metals and particularly for Zn. Finally, detailed metal immission maps (at 500 x 500 m block resolution) were created. To the best of our knowledge this is the first time that such maps are created based on a plant biomonitoring approach.

2. MATERIALS AND METHODS

2.1. Study area and sampling description

Zaragoza (NE Spain, 700,000 inhabitants) is located in a river valley. It presents an annual average temperature of 15°C and a precipitation of 367 mm with a mean relative humidity of 67%. It is a very sunny city (2,824 h $year^{-1}$), situated at 200 m above sea level and influenced by the Mediterranean Sea and the Atlantic Ocean. A wind called *Cierzo* is predominant and blows regularly from North-West to South-East direction. The data of the districts population density has been obtained from the web of the city (https://www.zaragoza.es/sedeelectronica/).

N. oleander is widely distributed in Zaragoza. Plants were sampled during July 2011 at 118 locations including the city center, in different industrial areas, around ring-roads, and in the outskirts (Fig. 1). All the 15 districts dividing the city were sampled: 18 plants were sampled at Actur (ACT), 10 at Casablanca (CAS), 6 at Casco (HIS), 13 at Centro (CEN), 9 at Delicias (DEL), 8 at Rabal (RAB), 4 at Almozara (ALM), 5 at Fuentes (FUE), 3 at Miralbueno (MIR), 3 at Oliver (OLI), 8 at San Jose (JOS), 12 at Santa Isabel (ISA), 6 at Torrero (TOR), 11 at Universidad (UNI), and 2 in rural outskirts (RUR), see district distribution in Fig. 1.

About 50 g of fresh, mature leaves were cut off from each plant from all sides of the canopy at 1.5 m above the ground level. This height was selected considering the maximum plant height (about 3 m) and the fact that they are regularly pruned to control height and diameter. This height is also of easy access and it is coincident with the maximum crown diameter of the plants. Moreover, similar studies found that road traffic derived metals as Pb and Fe accumulated preferentially at plant leaves located at 0.3 and 1.5-2 m; this last values are within the adult head height range [29]. Once at the laboratory, leaf samples were split in two subsamples, one of which was carefully washed with 0.1 M EDTA to remove surface dust and metals. Both subsamples, washed and unwashed, were dried for 48 h at 70 °C (to determine dry weight), ground, and stored until analysis.

2.2 Metal analysis

For the concentration analysis, 100 mg of material (from unwashed and washed plants) and 5 mL mixture of hydrochloric-nitric acid (4:1) were digested in an open vessel microwave digestion system (UltraCLAVE Milestone microwave) for 20 minutes at 220°C [17]. A mixture of 4 ml of HNO_3 69% PA- ISO and 1 ml of H_2O_2 (wt 33%) was added to samples. Metals were determined by simultaneous inductively coupled plasma (ICP-OES, Mod. ICAP 6500 DUO THERMO). Calibration curves were performed using standard stock solutions 1.0 mg l^{-1} diluted in 10% nitric acid. Recovery for metals ranged from 80% (Cr, Pb) to 92% (Zn). The detection limit for all metals was established at 0.5 mg kg^{-1} dry weight.

To discriminate anthropogenic from natural sources in the leaves of *N. oleander*, enrichment factors (EF) were calculated**:**

$$EF = [metal/Al]_{sample} / [metal/Al]_{upper\ continental\ crust}$$

Aluminium was used because of (a) its higher concentrations in plants compared to other lithogenic elements, (b) its low detection limits using plasma source mass spectrometry, and (c) it has no large contributions from anthropogenic sources, making it an ideal 'lithogenic' reference element. The metal/Al ratios for upper continental crust were taken from [30]. If the EF approaches value of 1, natural mineral dust from upper continental crustal material is likely to be the predominant source for element; if the EF is higher than 10, the element has a significant fraction contributed by anthropogenic ones [31]. It is worthwhile to mention that many metal/Al ratios are higher in soils than in upper continental crust (thus many people use rather soils) – but following previous findings, EF > 10 are robust evidences of the anthropogenic origin of the materials [32].

2.3 Zinc concentration and isotope ratios

Plants from nine sites belonging to three potentially different exposure scenarios were selected for Zn isotope analysis (see Fig. S6, S.I.): city center (mainly exposed to traffic), industrial areas (exposed to industrial emissions as combustion and metal related industries), and outskirts (cleanest sites exposed to transport from long-range aerosol sources). The samples were selected to represent a wide range of internal leaf Zn concentrations (9-76 mg kg^{-1}). The material (350 mg of leaf dry weight) was digested at 90˚C in HNO_3:H_2O_2 (1:1 v/v, products described in the point 2.2), then 1 ml of 40% hydrofluoric acid (Suprapur, Merck) was added and material was digested for 2 h at 90˚C. Digests were evaporated to dryness on a hotplate at 120˚C and the residues were dissolved in 3 ml of 7 M HCl. This protocol has been tested in previous studies [33].

Each solution was split into three aliquots: 1 ml for Zn concentration measurements, 1 ml for Zn isotope analysis, and 1 ml for archive. The first aliquot was made up to 3.5 ml of 1 M HCl prior to concentration measurements on a Varian VISTA PRO inductively coupled plasma atomic emission spectrometer (ICP-AES), with typical precision <5%. Zinc isotopes were analyzed in 0.1 M HNO_3 using a multi-collector inductively coupled plasma mass spectrometer (HR Nu Plasma, Nu Instruments, Wrexham, UK). Accuracy of the isotope measurements was assessed by the analysis of two in-house single element solutions (Imperial [34] and London Zn [35]), a plant certified reference material (BCR-62, olive leaves), and an in-house plant standard (HRM-14, grass). For details see Tab. S1 in the Supporting Information. The typical error (expressed as 2σ standard deviation) was ±0.12‰, and the procedural blank contributions were ≈4 ng of Zn.

The $\delta^{66}Zn$ was calculated using the following equation:

$$\delta^{x}\mathrm{Zn} = \left[\left(\frac{\frac{^{x}Zn}{^{64}Zn}}{\frac{1}{2}\left[\left(\frac{^{x}Zn}{^{64}Zn} \right)_{\mathrm{Standard1}} + \left(\frac{^{x}Zn}{^{64}Zn} \right)_{\mathrm{Standard2}} \right]} \right) - 1 \right] \times 1000$$

The δ^{66}Zn values in this study are normalized to JMC Lyon Zn (batch 3-0749L). Sample-standard bracketing was used to correct for instrumental mass bias [34] (more details on Fig. S1 in supporting information). Interferences were assessed plotting conventional three-isotopes plots using ^{64}Zn, ^{66}Zn, and ^{68}Zn from all samples. The regression line (R^2 0.96, n=73) intercepted within error (CI 95%) at y=0 and the slope varied within error (±2σ) of the theoretical slope of 2.00096 [36]. The δ^{66}Zn values from[21] cited in Fig. 4 have been converted to JMC using the equation (Criss 1999):

$$\delta \mathrm{X}_{\mathrm{Lyon}} = \delta \mathrm{X}_{\mathrm{st}} + \delta \mathrm{St}_{\mathrm{Lyon}} + \frac{1}{10^{3}} (\delta \mathrm{X}_{\mathrm{st}}) \cdot (\delta \mathrm{St}_{\mathrm{Lyon}})$$

In this expression, δX_{Lyon} is the δ^{66}Zn of the sample "X" relative to JMC, $\delta^{66}X_{st}$ is the δ^{66}Zn of the same sample relative to the standard "St", and δSt_{Lyon} is the δ^{66}Zn of the same standard relative to JMC. To convert the data we have used the δSt_{Lyon} provided by the authors. This was of 0.044±0.035‰[21] or 0.09±0.05‰ (Gioia et al 2008) for the in-house standard Johnson-Matthey Purontronic™ Batch NH 27040 [21], and a calculated offset of 0.32‰ for IRMM standard (Ochoa et al 2015; Ochoa and Weiss 2016).

2.4 Data analysis and representation

The different metal concentrations will be operationally defined as: total metal (analyzed from unwashed leaf material), internal metal (analyzed in washed leaf material), and external metal (calculated as the *total metal* minus the *internal metal*). The spatial distribution of these different metal concentrations (for Al, Cr, Cu, Ni, Pb, and Zn) in the leaves of *N. oleander* in Zaragoza has been mapped by geostatistical interpolation using Arc-Gis 9.3 software. Two-dimensional ordinary block kriging as a most advantageous interpolation technique [37], was applied to produce regular grids of 500 x 500 m. Statistical analyses (Pearson Correlation or T-student test) were carried out by using SPSS 10.0.

Previous studies (using principal component and cluster analysis) demonstrated that the presence of certain metals, such as Cu, Pb, and Zn, in urban environments, showed different associations with the major lithogenic elements as Al, Ca, Fe, Mg, and Mn [38]. Therefore, factor analysis (using SPSS 10.0) was used to identify the metal associations as an explanatory tool for the metal sources. Varimax rotation with Kaiser Normalization was used, followed by the extraction of the eigenvalues and eigenvectors from the correlation matrix. The KMO (Kaiser–Meyer–Olkin) test value (0.591) and Bartlett's test value of sphericity (245.509) show that the contaminant metals concentrations data of unwashed leaves of *N. oleander* from Zaragoza are suitable for factor analysis.

Annual average daily traffic –AADT, expressed as Σ vehicles year/365 days- was obtained from the Zaragoza City Environment Office. AADT values were available for 80% of the plants sampling locations. For the rest, AADT was estimated from the closest available locations (usually 2-4 values were used for calculations). Pearson correlations were used to test the influence of the traffic on metal present in *N. oleander* leaves.

3. RESULTS

3.1. Total metal concentrations in *N. oleander* leaves. The total metal concentrations for all the plants sampled in each city district are shown in Tab. S2A (S.I.); maps (for Cr, Ni, Pb, and Zn) are shown in Fig. S5 (S.I.). **Aluminum:** Plants with the highest concentrations of Al were sparsely distributed throughout the urban area, even at 6 km distance from center. The districts presenting the highest average total Al and the maximum concentrations were DEL (264 μg g^{-1}), CAS, and FUE (240-250 μg g^{-1}). The CAS and FUE districts are not adjacent to the city center; differently DEL is located very close and upwind from the center. The three districts with lowest Al concentrations were TOR, RAB, and ACT, located in a lateral or downwind position from the city center. **Copper**: Plants with the highest averaged total concentration of Cu were located in CEN and HIS, both belonging to the city center, ranging between 6.93 and 13.79 μg g^{-1}. The maximum Cu concentration was found in the western part of the city, in the DEL district (37.71 μg g^{-1}). The lowest concentration was found in the ACT district (2.46 μg g^{-1}), northern of the city and farther from the center. **Chromium:** The highest averaged total concentrations of Cr were found in plants located in the districts of CEN, HIS, and DEL, ranging between 1.28 and 1.56 μg g^{-1}. The Cr concentration in leaves was elevated in the western districts (see Fig. S5, S.I.). By contrast, concentrations were lower than 0.50 μg g^{-1} in the southern regions, TOR and RUR districts both far from the city center (<6km). **Nickel:** The Ni concentration increased from 0.39 μg g^{-1} in the western peripheral districts (ISA) to 1.3 μg g^{-1} in the eastern ones (DEL and CEN, see Fig. S5, S.I.). Ni was the metal showing the lowest concentration in the leaves of the city, with a maximum 6 μg g^{-1} and a minimum 0.1 μg g^{-1}. **Lead:** Average concentration for Pb ranged between 0.29 and 2.78 μg g^{-1} (OLI and DEL districts respectively). The districts with highest values were HIS, DEL, and CEN (ranging between 1.7 and 10 μg g^{-1}). The districts with lowest concentrations were MIR and OLI (around 0.3 μg g^{-1}). Both districts are peripheral to the city and the most upwind of all districts (see details in Fig. S5, S.I.). **Zinc:** Zinc concentrations were highest (227.11 μg g^{1}) in the city center (HIS). Compared to the other metals, Zn was present in all districts and at higher concentrations than other metals (see Fig. S5, S.I.). The average values ranged between 25.33-60.70 μg g^{-1}, being the highest values measured. Concentrations of Zn decrease in the east or downwind direction, being JOS and RAB, both of them located 4km from the city center, the districts less affected by Zn.

3.2. Internal metal concentrations in *N. oleander* leaves. Internal metal concentrations (Fig. 2.) showed a similar spatial distribution as total metal content (Fig. S5, Tab. S2.A, S.I). The highest internal metal concentrations of Cr and to a lesser extent of Ni and Pb were found in plants located along to the main wind pathway (that of the *Cierzo*, blowing regularly from North-West to South-East direction). **Aluminum:** Plants with highest concentrations of Al were

sparsely distributed throughout the urban area, even at 6 km distance from center. The districts presenting the highest average total Al were FUE, CAS, and JOS; all three are peripheral to the city center. The three districts with lowest concentrations were MIR, RAB, and ACT, also peripheral. **Copper**: The maximums were located in CEN and HIS, both at the city center. The minimum was found in the ALM district. However, the differences between the maximum and minimum values were really narrow. **Chromium:** The highest averaged total concentrations of Cr were found in plants located in the districts of CEN, HIS, and DEL. Again, the differences between extreme values were narrow. **Nickel:** The maximums were found at CAS, CEN, and MIR, while the minimum was found far from the city center, at ISA district. **Lead:** City center districts presented the highest values (HIS, DEL, and CEN, ranging between 1 and 1.56 μg g^{-1}), while the lowest ones were detected in the peripheral districts (ACT, MIR, and OLI). **Zinc:** The average values ranged between 25 and 45.70 μg g^{-1}. The maximums were detected at ALM and HIS districts (45 μ g^{-1}). Concentrations of Zn decreased in the East or downwind direction, hence the lowest levels of Zn were found in the peripheral districts as JOS and RAB.

3.3. External metal concentrations in *N. oleander* plants. Metal adsorption onto the external surfaces of the leaves has been calculated as the difference between unwashed and washed leaves. These results are shown in Tab. S2B (S.I), and are attributed to the atmospheric deposition from the surroundings. Significant differences ($p<0.05$) were found between washed and unwashed leaves for Al, Cr, and Pb content. The washing removed, in average, 27 % of the total Al, 22 % of the Cr, 15 % of the Cu, 16 % of the Pb, and 8 % of the Zn. Leaves from city centre districts (HIS and DEL) presented the highest amount of metals deposited (Zn, Cu, Ni, and Pb, see in Tab. S2.A, S.I). The peripheral district of TOR presented the lowest accumulation for most metals.

3.4. Enrichment Factors. Calculated enrichment factors are shown in Table S2 (S.I.). We discuss only the enrichment factors for washed leaves (i.e. the metal contained in the plant tissues), because these are the values used for monitoring purposes. The highest EF for Cr were in samples from the CEN and HIS districts (EF of 21-23 respectively), both located at the city center. Plants located in the CAS and RUR districts, at the outskirts of the city, have lowest values (around 6). The highest EF for copper (361) were found in plants located in the MIR district, upwind from the city center, while the lowest values (123-155) were found across the whole city: ALM, CAS, FUE, and JOS districts. The EF for Ni ranged between 30 and 10, presenting a spatial distribution similar to Cu. Plants with the highest Pb EF (36-39) were in the central districts of HIS, CEN, and DEL, where the traffic is most intense. The Pb values in those districts were at least twice as high as in the rest of the city. The highest EF values for Zn were found in districts of HIS and MIR (456-413), while the lowest ones (170-180) were measured at FUE and JOS, the two most downwind districts of the city.

3.5. Zinc isotopes. The $\delta^{66}Zn_{Lyon}$ of *N. oleander* leaves ranged between -0.95 and 0.70 ‰, likely reflecting different sources of Zn. Isotopically heaviest Zn was found in the North of the city (0.70 ‰) and close to the main industrial hotspots (samples 5 and 7, see Figure S6, S.I.), while the lightest signatures (-0.95 ‰) were found away from both city centre and industries (Fig. 3B). We found no significant difference between the zinc isotope signatures of washed and

unwashed subsamples (Table S3, S.I.).

3.6. Factor analysis. The calculations of the factors loadings with a varimax rotation, as well as the eigenvalues and communalities are shown in Table S4 (S.I.). The results indicate that first three factors extracted accounted for 71% of the total variance. The highest percentage of variance (30%) was explained by a component with high loadings on Al, Pb, Cr, and Ni. The second component accounted for 23% of the variance was related to Cu and Zn. The third component explained 19% of the variance and was related to Ce.

3.7. Traffic occurrence vs. metal in leaves of *N. oleander*. The influence of traffic on the metals accumulated by plants was assessed by fitting linear regression models. The best fitting, for all metals, was found when integrating the data at district scale: the sum of the traffic prevailing at each location (i.e traffic emissions at which plants have been potentially exposed) vs. the sum of the metals –total concentrations- accumulated by these leaves (see Fig. S3, S.I.). The traffic explained between 82-68% of the metals most correlated with that source accumulated by leaves (Cr, Cu, Zn, and Ni, see details in Fig. S3, S.I.). The Ce was the metal presenting a weaker correlation with traffic (≈ 0.4 R^2), whereas Pb presented an intermediate value (≈ 0.5 R^2) compared to the most traffic-related metals.

4. DISCUSSION

4.1. Metal concentration in the leaves of *N. oleander*

Plants leaf tissue has been used as biomonitoring tool for aerial pollution [9, 20, 31, 39-42]. Our results in metal content in *N. oleander* are in agreement with previous studies, especially for Al, Cu, Cr, and Zn [9, 17]. The only metal presenting different concentrations is Pb; our results averaged 0.6 mg kg^{-1} while older studies performed in 1998-2000 [17] found averages around 10 times higher (4.9 mg kg^{-1}). This can be explained because leaded gasoline was withdrawn entirely from the European Union on 1 January 2000, causing a noticeable reduction on lead present in urban environments [43].

The % of metals removed by washing (from 8% for Zn to 27% for Al) was within the range found in previous studies [9, 17]. As shown in Table S2A and S2B, significant differences on metal content (Al, Cr, Cu, and Pb) between washed and unwashed leaves confirms that part of the heavy metal present in leaves proceeded from atmospheric deposition. The amount of contaminants that penetrates into leaves varies with species and metal. For example, Cd and Cu penetrate easily into the leaf, while Pb is mostly adsorbed to the epicuticular lipids at the surface [44]. Zinc may be retained in the epicuticular lipids at the surface on the unwashed leaves [15]. Other chemical elements such as such as sulphur (SO_2) and nitrogen (NO_x) have been described to cross the stomata and reach the mesophyll [45, 46] where they are accumulated and might induce oxidative stress damage [12]. The leaves of *N. oleander* are smooth with a thick cuticle covered by numerous stomata, grouped in sunken hairy pockets [17] that are, potentially, the main exposure way for internal leaf tissues to PM. The figure S4 (S.I.) shows images taken from scanning electron microscopy and EDAX analysis that confirmed the presence of metal-containing PM (ranging from <1 to 6 µm, thus belonging to the PM10 and PM2.5 fractions) in the surfaces and stomata crypts of leaves collected in this study.

393
394 **4.2. Enrichment factors as indicator of anthropogenic origin of metals**
395 All studied samples (15) presented enrichment (EF>10) in Zn and Cu, while 14 samples were
396 enriched in Ni, 13 in Pb, and 9 in Cr (Tab. S2B). Copper and Zn presented the highest EF. The
397 values clearly suggest the anthropogenic origin of the metals found in the plants.
398
399 The PCA allowed identifying metal associations as an explanatory tool for inferring metal
400 sources. Three factors accounted for 71% of the accumulative variance (Tab. S4). The highest
401 percentage of variance (30%) is explained by a component with high loadings on Al, Pb, Cr, and
402 Ni. The last three are associated with traffic and industrial sources (metal work related
403 industries), while Al is commonly associated with lithogenic elements [17]. Therefore, soil dust
404 and wind re-suspension were, most probably the sources for these elements. The second
405 component accounted for 23% of the variance, was related to Cu and Zn, and might be
406 associated with industrial sources [19]. The third explaining 19% of the variance was related to
407 Ce and can be associated to traffic [47].
408
409 **4.3. Isotopic signature of Zn and possible link to sources**
410
411 The isotopic composition of the Zn ($\delta^{66}Zn_{Lyon}$) found on unwashed *N. oleander* leaves showed a
412 wide range of variation, from -0.85 to 0.70‰. This range is similar to previous data on leaves
413 from several species growing in a pristine environment ($\delta^{66}Zn_{Lyon}$ -0.91 to 0.63‰)(Viers et al
414 2007).However, all samples in our study had an EF>10 indicating a strong contribution from
415 anthropogenic sources. Moreover, our lineal model shows that about 70% of the variation in
416 Zn concentration can be explained by traffic intensity, and fine PM containing metals were
417 found in the stomatal chambers. Isotopic signatures (Fig. 4) and their relationship with the
418 distance to metal industries (galvanization, electroplating, and foundry) and the predominant
419 winds (Fig. 3A), may indicate the importance of industrial sources of Zn and of the wind as
420 main spreading factor. Few samples may have lithological origin (Fig. 4), or from a mixture of
421 industrial activities and long-range airborne transport of sediments and other materials as
422 ores, rainfall, etc (Fig. 4). These results are in agreement with studies showing that Pb and Cu
423 accumulated by *N. oleander* is related to the distance from industrial hotspots [18].
424
425 The heaviest signatures were those from samples 5 and 7 (0.48 and 0.70‰, respectively),
426 taken right from the industrial hotspot to the north of the city (ISA district). Values were
427 similar to those of industries related with galvanized hardware (Fig. 4). Aerosols collected at a
428 short distance (190-1250 m) from a Pb-Zn refinery in France showed a high proportion of
429 PM>10 and $\delta^{66}Zn_{Lyon}$ of 0.02 to 0.19‰, closely matching those of the ore (0.1-0.22‰)[54]. The
430 signature was attributed to resuspension from the slag heaps and local working units of the
431 refinery, and a similar process could explain the isotopic signatures of samples 5 and 7. By
432 contrast, aerosols taken at a higher distance (1720 to 4560 m) were mostly composed of
433 PM10, and their isotopic composition was lighter (-0.52 to -0.02‰)[54]. This enrichment of the
434 light isotopes was attributed to emissions from the main chimney, since the dust collected
435 from it had a $\delta^{66}Zn$ of -0.67‰. Isotopic fractionation during coal combustion leads to the
436 enrichment of heavy isotopes in the fly ashes with respect to the fuel, while the lighter
437 isotopes would be enriched in the vapor phase (Ochoa and Weiss 2015). Samples 1, 2, and 4 in

our study, collected at around 2 Km distance from the galvanizing industry, are in a similar range to the aerosols in [54] (-0.31 to 0.07‰). Besides, PM in the leaves of *N. oleander* in this study were <6 µm. We propose that the isotopic composition of Zn in samples 1, 2, and 4 could be the result of isotopic fractionation during high temperature processes in the galvanizing industry, and subsequent transport of the resulting fine PM with the wind. This indicates that the contribution of galvanic industries to the total metal emissions in Zaragoza is significant and confirms Zn stable isotopes as a reliable tracer of emissions sources.

The size of the particles appears determinant for the Zn isotopic signature, and particles of different sizes might come from separate sources. The $\delta^{66}Zn_{Lyon}$ of PM <10 µm from São Paulo (Brazil) was in the range -1.13 to -0.46‰ and that of gasoline was approximately -0.6 to -0.3‰, so the isotopic signature of the aerosols was attributed to traffic (Gioia et al 2008). In addition, PM_{10} from aerosols in Barcelona (Spain) were in the range -0.83 to -0.45‰ and probably originated from combustion, while PM_{80} from London (UK) were isotopically heavy (0.03 to 0.49‰) and were ascribed to non-exhaust traffic emissions, likely from tire wear (Ochoa et al 2016). In a recent study, fine PM from London yielded lighter $\delta^{66}Zn_{Lyon}$ (-0.21 to 0.33‰) (Dong et al 2017) than the PM_{80} in the previous study.

Taking together all the above information, it appears that Zn pollution related to traffic can be divided into two distinct sources: the PM originated from combustion, which are usually fine (<10 µm) and isotopically light, and the PM from non-exhaust emissions like tire wear, generally coarse (>10 µm) and isotopically heavy. In our study, samples 3 and 9 are closer to the central district and showed $\delta^{66}Zn_{Lyon}$ of 0.31 and 0.47‰ respectively, consistent with substantial contribution from non-exhaust emissions. By contrast, samples 6 and 8 were farther away from the city centre and industrial areas, and their isotopic signatures (-0.18‰ and -0.85‰ respectively) are probably the least influenced by anthropogenic contribution.

The fact that there were no significant differences on isotopic composition between washed and unwashed leaves for each sample indicates that Zn isotopic composition of the *N. oleander* leaves may be a reliable picture of the Zn exposure scenario at medium and long term. Moreover, differences in Zn isotopic signature between leaves may be attributed to differences in the source of Zn.

4.4. External metal –immission- accumulated on *N. oleander* leaves

The Cr immission ranged between 0.01 (TOR district) and 0.55 mg Kg^{-1} leaf biomass (OLI). Zinc showed the highest immision at city centre (HIS, with 15 mg Kg^{-1}) while the southern and most downwind district, JOS, presented the lowest value (0.51). The highest amount of Al immitted was measured in MIR and DEL districts (105-123 mg per Kg^{-1} of leave biomass respectively, Tab. S2B). DEL district, similarly, presented the highest immission for Ni (0.79 mg Kg^{-1}), Pb (1.22 mg Kg^{-1}), and Cu (3.54 mg Kg^{-1}). In general, plants presenting the highest level of metal immission were located in DEL district. This district is the most populated of the region (340 people ha^{-1}), even more than the centre (333 people ha^{-1}), and has an intense traffic (it is the Northern entrance of road traffic into the city). In general, Pb and Cu showed greater immission close to the city centre (DEL, CEN, and HIS districts), while Ce and Cr were much more widely dispersed, showing high values in locations sparsely distributed. Differently to these spatial patrons, Ni and Al showed two clear “hotspots”, probably associated to punctual sources of such metals.

4.5. Metal content on *N. oleander* leaves

The Al concentration increased 3 times from 87 μg g^{-1} in the rural spots to 264 μg g^{-1} in the district DEL (Tab. 2). Similar trends were found for Ni (1.3-2.8 μg g^{-1}) and Pb (0.3-0.4 μg g^{-1}). Plants presenting the highest concentration of metals (Al, Ni and Pb) were located in Delicias (DEL). The Cr concentration ranged between 1.28 and 1.56 μg g^{-1} in the city centre and remained elevated in the NO districts, whereas concentrations were lower than 0.50 μg g^{-1} in the south. Zinc concentrations ranged from 25.33 to 60.70 μg g^{-1}.

In Zaragoza, median concentrations of trace elements in leaves of *N. oleander* were distributed in the following order: Al>Zn>Cu>Pb>Cr>Ni>. This order is similar to that measured in other similarly sized cities as Metz in France [51] or Livorno in Italy [52]. Plants in Zaragoza presented higher concentrations of Pb than in Sevilla (Spain) [16] and Palermo in Italy [17], and higher Zn, Cu, and Ni than Antalya in Turkey [9]. Comparing Zaragoza with other heavily industrialized areas, Pb and Cu concentrations measured in leaves of *N. oleander* in Huelva (SW, Spain), were higher than those found in Zaragoza [18]. However, it should be warned that the information about the "immision scenario" derived from metals deposited in the leaf surfaces can be modified by events as rains, traffic alterations by road works, or plant pruning.

Acknowledgements

We tank Graziella Berta and Simone Cantamessa (Dipartimento di Scienze dell'Ambiente e della Vita, Università del Piemonte Orientale Amedeo Avogadro, Italia) for the EDAX analysis shown at Supporting Information. This work has been supported by the regional Aragon Government (Consolidated Applied Research Group ref. E61, and the Research Project ref. PI067/09 of the Call for Research Funding 2009 of the Aragon Government) and by Spanish Ministry of Economy and Competitiveness (National Research Plan, ref. BFU2010-22053). The research leading to these results has received funding from the People Programme (Marie Curie Actions) of the European Union's Seventh Framework Programme FP7/2007-2013/ under REA grant agreement n° 299473.

References

1. Richter, D.; Peter Williams, W. *Assessment and Management of Urban Air Quality in Europe*; European Environment Agency: Europe, 1998; p 150.
2. Nordberg, G. F.; Fowler, B. A.; Nordberg, M., *Handbook on the Toxicology of Metals*. Academic Press: 2015; Vol. I. General Considerations.
3. Schwartz, J.; Neas, L. M., Fine Particles Are More Strongly Associated than Coarse Particles with Acute Respiratory Health Effects in Schoolchildren. *Epidemiology* **2000,** *11*, (1), 6-10.
4. Adriano, D. C., *Trace Elements in Terrestrial Environments: Biogeochemistry, Bioavailability, and Risks of Metals*. Springer: 2001; p 888.
5. Nriagu, J. O.; Pacyna, J. M., Quantitative assessment of worldwide contamination of air, water and soils by trace metals. *Nature* **1988,** *333*, (6169), 134-139.
6. Kampa, M.; Castanas, E., Human health effects of air pollution. *Environmental*

Pollution **2008,** *151*, (2), 362-367.
7. Spiro, B.; Weiss, D. J.; Purvis, O. W.; Mikhailova, I.; Williamson, B. J.; Coles, B. J.; Udachin, V., Lead isotopes in lichen transplants around a Cu smelter in Russia determined by MC-ICP-MS reveal transient records of multiple sources. *Environ. Sci. Technol.* **2004,** *38*, (24), 6522-6528.
8. Dongarra, G.; Sabatino, G.; Triscari, M.; Varrica, D., The effects of anthropogenic particulate emissions on roadway dust and Nerium oleander leaves in Messina (Sicily, Italy). *J. Environ. Monit.* **2003,** *5*, (5), 766-773.
9. Aksoy, A.; Ozturk, M. A., Nerium oleander L. as a biomonitor of lead and other heavy metal pollution in Mediterranean environments. *Science of the Total Environment* **1997,** *205*, (2-3), 145-150.
10. Mulgrew, A.; Williams, P. Biomonitoring of air quality using plants. http://www.opengrey.eu/item/display/10068/234928
11. Kozlov, M. V.; Haukioja, E.; Bakhtiarov, A. V.; Stroganov, D. N.; Zimina, S. N., Root versus canopy uptake of heavy metals by birch in an industrially polluted area: contrasting behaviour of nickel and copper. *Environmental Pollution* **2000,** *107*, (3), 413-420.
12. Robinson, M.; Heath, J.; Mansfield, T., Disturbances in stomatal behaviour caused by air pollutants. *Journal of Experimental Botany* **1998,** *49*, 461-469.
13. McAinsh, M.; Evans, N.; Montgomery, L.; North, K., Calcium signalling in stomatal responses to pollutants. *New Phytologist* **2002,** *153*, (3), 441-447.
14. Pourkhabbaz, A.; Rastin, N.; Olbrich, A.; Langenfeld-Heyser, R.; Polle, A., Influence of Environmental Pollution on Leaf Properties of Urban Plane Trees, Platanus orientalis L. *Bulletin of Environmental Contamination and Toxicology* **2010,** *85*, (3), 251-255.
15. Al-Shayeb, S. M., Comparison study of Phoenix dactylifera L. and Nerium oleander L. as biomonitors for lead and other elements. *Asian Journal of Chemistry* **2002,** *14*, (2), 597-601.
16. Fernández Espinosa, A. J.; Oliva, S. R., The composition and relationships between trace element levels in inhalable atmospheric particles (PM10) and in leaves of Nerium oleander L. and Lantana camara L. *Chemosphere* **2006,** *62*, (10), 1665-1672.
17. Mingorance, M. D.; Oliva, S. R., Heavy metals content in N-oleander leaves as urban pollution assessment. *Environmental Monitoring and Assessment* **2006,** *119*, (1-3), 57-68.
18. Mingorance, M. D.; Valdes, B.; Oliva, S. R., Strategies of heavy metal uptake by plants growing under industrial emissions. *Environment International* **2007,** *33*, (4), 514-520.
19. Oliva, S. R.; Mingorance, M. D., Study of the impact of industrial emission on the vegetation grown around Huelva (South of Spain) City. *Journal of Atmospheric Chemistry* **2004,** *49*, (1-3), 291-302.
20. Verma, D. K.; Gupta, A. P.; Dhakeray, R., Bioindicators: A Comparative Study on Uptake and Accumulation of Heavy Metals in Some Plant's Leaves of MG Road, Agra City, India. **2010**.
21. Larner, F.; Rehkämper, M., Evaluation of Stable Isotope Tracing for ZnO Nanomaterials—New Constraints from High Precision Isotope Analyses and Modeling. *Environ. Sci. Technol.* **2012,** *46*, (7), 4149-4158.
22. Cloquet, C.; Carignan, J.; Lehmann, M. F.; Vanhaecke, F., Variation in the isotopic composition of zinc in the natural environment and the use of zinc isotopes in biogeosciences: a review. *Analytical and Bioanalytical Chemistry* **2008,** *390*, (2), 451-463.

23. Cloquet, C.; Carignan, J.; Libourel, G., Isotopic Composition of Zn and Pb Atmospheric Depositions in an Urban/Periurban Area of Northeastern France. *Environ. Sci. Technol.* **2006,** *40*, (21), 6594-6600.
24. Dolgopolova, A.; Weiss, D. J.; Seltmann, R.; Kober, B.; Mason, T. F. D.; Coles, B.; Stanley, C. J., Use of isotope ratios to assess sources of Pb and Zn dispersed in the environment during mining and ore processing within the Orlovkaâ€“Spokoinoe mining site (Russia). *Applied Geochemistry* **2006,** *21*, (4), 563-579.
25. Weiss, D. J.; Rausch, N.; Mason, T. F. D.; Coles, B. J.; Wilkinson, J. J.; Ukonmaanaho, L.; Arnold, T.; Nieminen, T. M., Atmospheric deposition and isotope biogeochemistry of zinc in ombrotrophic peat. *Geochimica et Cosmochimica Acta* **2007,** *71*, (14), 3498-3517.
26. Gonzalez, R.; Strekopytov, S.; Amato, F.; Querol, X.; Reche, C.; Weiss, D., New Insights from Zinc and Copper Isotopic Compositions into the Sources of Atmospheric Particulate Matter from Two Major European Cities. *Environ. Sci. Technol.* **2016,** *50*, (18), 9816-9824.
27. López, J. M.; Callén, M. S.; Murillo, R.; García, T.; Navarro, M. V.; de la Cruz, M. T.; Mastral, A. M., Levels of selected metals in ambient air PM10 in an urban site of Zaragoza (Spain). *Environ Res* **2005,** *99*, (1), 58-67.
28. IAE Instituto Aragonés de Estadística. Área de emisiones a la atmósfera. http://www.aragon.es/DepartamentosOrganismosPublicos/Organismos/InstitutoAragonesEstadistica/AreasTematicas/MedioAmbiente/ci.04_Cambio-climatico_Emisiones-a-la-atmosfera.detalleDepartamento?channelSelected=c70d2135fc5fa210VgnVCM100000450a15acRCRD)
29. Maher, B. A.; Moore, C.; Matzka, J., Spatial variation in vehicle-derived metal pollution identified by magnetic and elemental analysis of roadside tree leaves. *Atmospheric Environment* **2008,** *42*, (2), 364-373.
30. Taylor, S. R.; McLennan, S. M., *The continental crust: Its composition and evolution*. Blackwell Scientific Publications: Osney Mead, Oxford, 1985; p Medium: X; Size: Pages: 328.
31. Tomašević, M.; Rajšić, S.; Đorđević, D.; Tasić, M.; Krstić, J.; Novaković, V., Heavy metals accumulation in tree leaves from urban areas. *Environmental Chemistry Letters* **2004,** *2*, (3), 151-154.
32. Weiss, D.; Shotyk, W.; Cheburkin, A. K.; Gloor, M.; Reese, S., Atmospheric lead deposition from 12,400 to Ca. 2,000 yrs BP in a peat bog profile, Jura mountains, Switzerland. *Water Air Soil Poll* **1997,** *100*, (3-4), 311-324.
33. Caldelas, C.; Dong, S. F.; Araus, J. L.; Weiss, D. J., Zinc isotopic fractionation in Phragmites australis in response to toxic levels of zinc. *Journal of Experimental Botany* **2011,** *62*, (6), 2169-2178.
34. Mason, T. F. D.; Weiss, D. J.; Horstwood, M.; Parrish, R. R.; Russell, S. S.; Mullane, E.; Coles, B. J., High-precision Cu and Zn isotope analysis by plasma source mass spectrometry - Part 2. Correcting for mass discrimination effects. *J Anal Atom Spectrom* **2004,** *19*, (2), 218-226.
35. Arnold, T.; Schonbachler, M.; Rehkamper, M.; Dong, S. F.; Zhao, F. J.; Kirk, G. J. D.; Coles, B. J.; Weiss, D. J., Measurement of zinc stable isotope ratios in biogeochemical matrices by double-spike MC-ICPMS and determination of the isotope ratio pool available for plants from soil. *Analytical and Bioanalytical Chemistry* **2010,** *398*, (7-8), 3115-3125.
36. Rosman, K. J. R.; Taylor, P. D. P., Isotopic compositions of the elements 1997. *J Anal Atom Spectrom* **1998,** *13*, (10), 45n-55n.
37. Navas, A.; Machin, J., Spatial distribution of heavy metals and arsenic in soils of

Aragon (northeast Spain): controlling factors and environmental implications. *Applied Geochemistry* **2002,** *17*, (8), 961-973.
38. Lee, C. S.; Li, X. D.; Shi, W. Z.; Cheung, S. C.; Thornton, I., Metal contamination in urban, suburban, and country park soils of Hong Kong: A study based on GIS and multivariate statistics. *Science of the Total Environment* **2006,** *356*, (1-3), 45-61.
39. Celik, A.; Kartal, A. A.; Akdogan, A.; Kaska, Y., Determining the heavy metal pollution in Denizli (Turkey) by using Robinio pseudo-acacia L. *Environment International* **2005,** *31*, (1), 105-112.
40. Keane, B.; Collier, M. H.; Shann, J. R.; Rogstad, S. H., Metal content of dandelion (Taraxacum officinale) leaves in relation to soil contamination and airborne particulate matter. *Science of the Total Environment* **2001,** *281*, (1â€“3), 63-78.
41. Sawidis, T.; Marnasidis, A.; Zachariadis, G.; Stratis, J., A Study of Air-Pollution with Heavy-Metals in Thessaloniki City (Greece) Using Trees as Biological Indicators. *Archives of Environmental Contamination and Toxicology* **1995,** *28*, (1), 118-124.
42. Suzuki, K.; Yabuki, T.; Ono, Y., Roadside Rhododendron pulchrum leaves as bioindicators of heavy metal pollution in traffic areas of Okayama, Japan. *Environmental Monitoring and Assessment* **2009,** *149*, (1-4), 133-141.
43. Llop, S.; Porta, M.; Martinez, M. D.; Aguinagalde, X.; Fernández, M. F.; Fernández-Somoano, A.; Casas, M.; Vrijheid, M.; Ayerdi, M.; Tardón, A.; Ballester, F., Estudio de la evolución de la exposición a plomo en la población infantil española en los últimos 20 años: ¿un ejemplo no reconocido de «salud en todas las políticas»? *Gac Sanit* **2013,** *27*, 149-155.
44. Greger, M., Metal Availability and Bioconcentration in Plants. In *Heavy Metal Stress in Plants*, Springer Berlin Heidelberg: 1999; pp 1-27.
45. Kabata -Pendias, A., *Trace Elements in Soils and Plants*. Press, C. R. C.: Boca Raón, Florida, EEUU, 2001; Vol. 3er.
46. RENGEL, Z., 11. MECHANISMS OF PLANT RESISTANCE TO TOXICITY OF ALUMINIUM AND HEAVY METALS. *Mechanisms of Environmental Stress Resistance in Plants* **1997**, 241.
47. Gantt, B.; Hoque, S.; Willis, R. D.; Fahey, K. M.; Delgado-Saborit, J. M.; Harrison, R. M.; Erdakos, G. B.; Bhave, P. V.; Zhang, K. M.; Kovalcik, K.; Pye, H. O. T., Near-Road Modeling and Measurement of Cerium-Containing Particles Generated by Nanoparticle Diesel Fuel Additive Use. *Environ. Sci. Technol.* **2014,** *48*, (18), 10607-10613.
48. Moynier, F.; Pichat, S.; Pons, M. L.; Fike, D.; Balter, V.; Albarede, F., Isotopic fractionation and transport mechanisms of Zn in plants. *Chem Geol* **2009,** *267*, (3-4), 125-130.
49. Weiss, D. J.; Mason, T. F. D.; Zhao, F. J.; Kirk, G. J. D.; Coles, B. J.; Horstwood, M. S. A., Isotopic discrimination of zinc in higher plants. *New Phytologist* **2005,** *165*, (3), 703-710.
50. Aucour, A. M.; Bedell, J. P.; Queyron, M.; Magnin, V.; Testemale, D.; Sarret, G., Dynamics of Zn in an urban wetland soil-plant system: Coupling isotopic and EXAFS approaches. *Geochim Cosmochim Ac* **2015,** *160*, 55-69.
51. Cloquet, C.; Carignan, J.; Libourel, G., Atmospheric pollutant dispersion around an urban area using trace metal concentrations and Pb isotopic compositions in epiphytic lichens. *Atmospheric Environment* **2006,** *40*, (3), 574-587.
52. Scerbo, R.; Possenti, L.; Lampugnani, L.; Ristori, T.; Barale, R.; Barghigiani, C., Lichen (Xanthoria parietina) biomonitoring of trace element contamination and air quality assessment in Livorno Province (Tuscany, Italy). *Science of the Total*

Environment **1999,** *241*, (1–3), 91-106.
53. John, S. G.; Genevieve Park, J.; Zhang, Z.; Boyle, E. A., The isotopic composition of some common forms of anthropogenic zinc. *Chem Geol* **2007,** *245*, (1–2), 61-69.
54. Mattielli, N.; Petit, J. C. J.; Deboudt, K.; Flament, P.; Perdrix, E.; Taillez, A.; Rimetz-Planchon, J.; Weis, D., Zn isotope study of atmospheric emissions and dry depositions within a 5 km radius of a Pb–Zn refinery. *Atmospheric Environment* **2009,** *43*, (6), 1265-1272.
55. Sivry, Y.; Riotte, J.; Sonke, J. E.; Audry, S.; Schäfer, J.; Viers, J.; Blanc, G.; Freydier, R.; Dupré, B., Zn isotopes as tracers of anthropogenic pollution from Zn-ore smelters The Riou Mort–Lot River system. *Chem Geol* **2008,** *255*, (3–4), 295-304.
56. Luck, J.; Othman, D. B.; Albarede, F.; Telouk, P., Pb, Zn and Cu isotopic variations and trace elements in rain. *Geochemistry of the Earth's Surface. Balkema, Rotterdam* **1999**.
57. Pichat, S.; Douchet, C.; Albarède, F., Zinc isotope variations in deep-sea carbonates from the eastern equatorial Pacific over the last 175 ka. *Earth and Planetary Science Letters* **2003,** *210*, (1–2), 167-178.
58. Maréchal, C. N.; Télouk, P.; Albarède, F., Precise analysis of copper and zinc isotopic compositions by plasma-source mass spectrometry. *Chem Geol* **1999,** *156*, (1–4), 251-273.
59. John, S. G.; Geis, R. W.; Saito, M. A.; Boyle, E. A., Zinc isotope fractionation during high-affinity and low-affinity zinc transport by the marine diatom Thalassiosira oceanica. *Limnol Oceanogr* **2007,** *52*, (6), 2710-2714.

References shown at Fig 4: [53], [49], [54], [55], [56], [57], [58], [23], [24], [22], [59]. NOTE: this info is needed in order to list all references using ENDNOTE Soft.

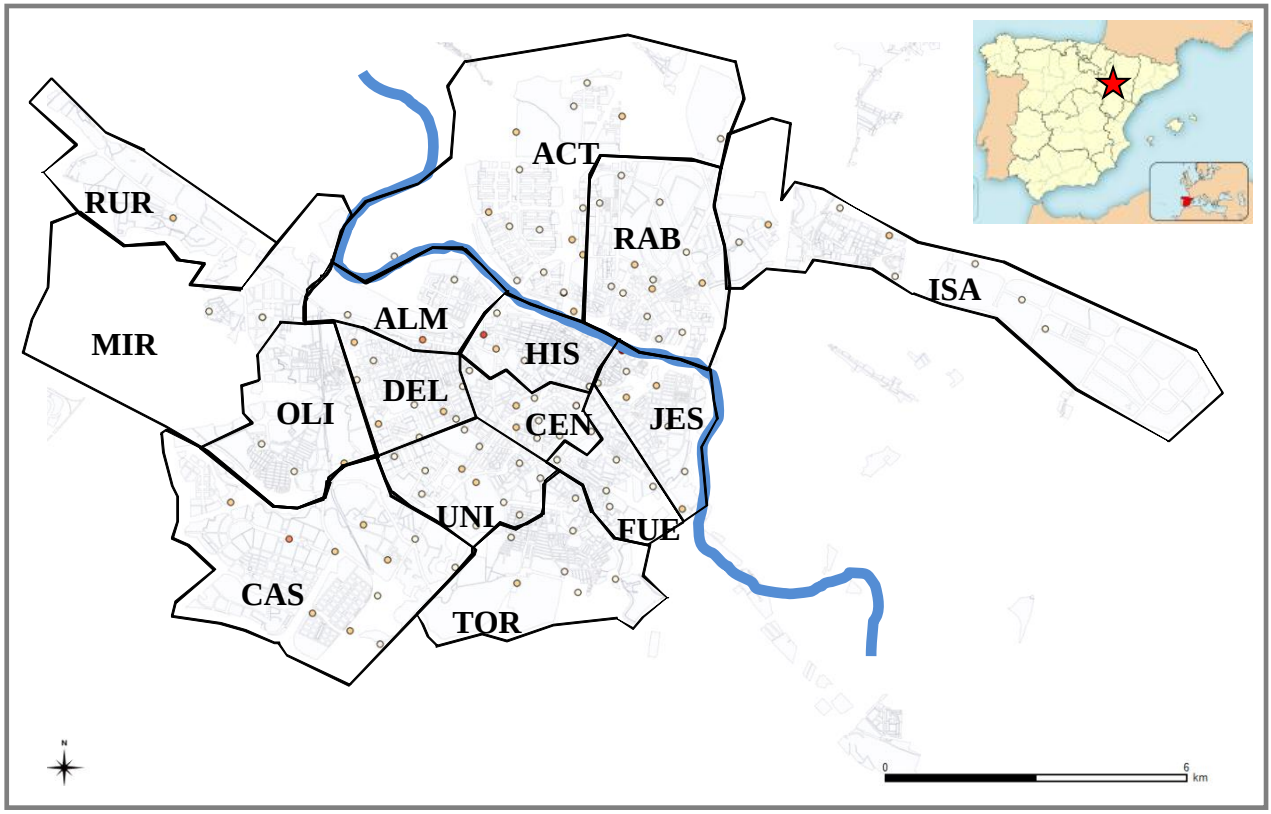

Figure 1. Location of Zaragoza (in Spain); city districts and location of the plants sampled in this study. The blue line represents the Ebro River.

731

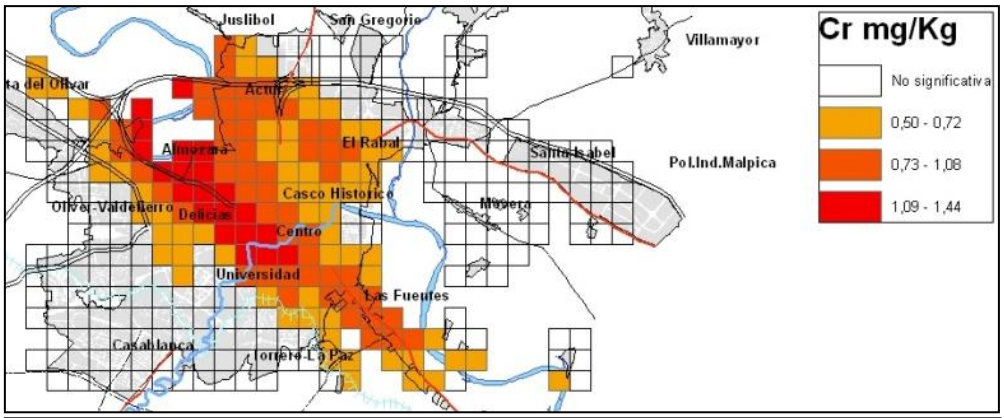

732

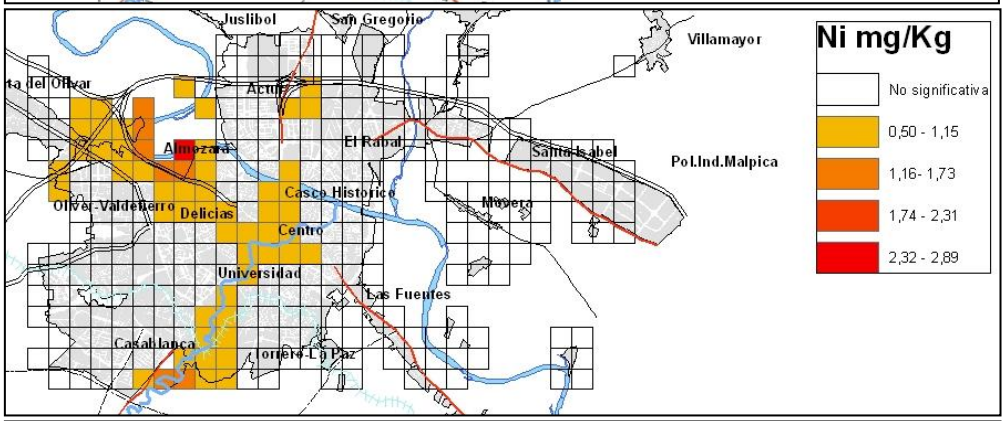

733

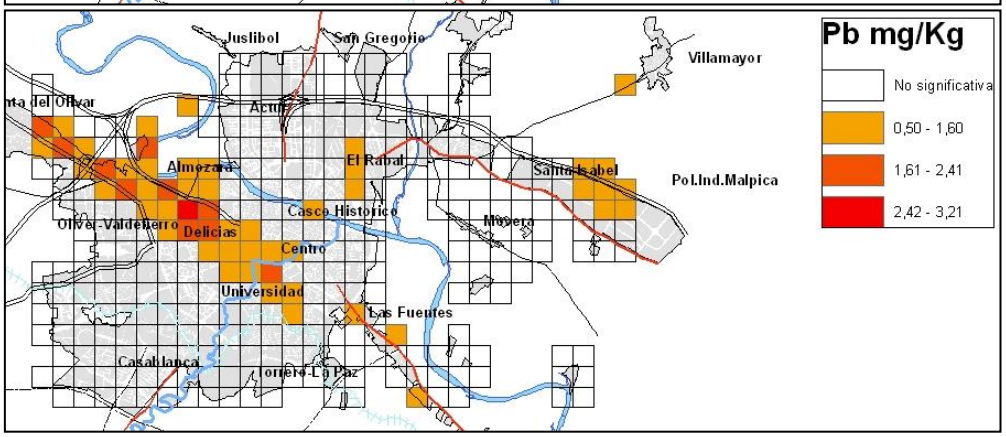

734

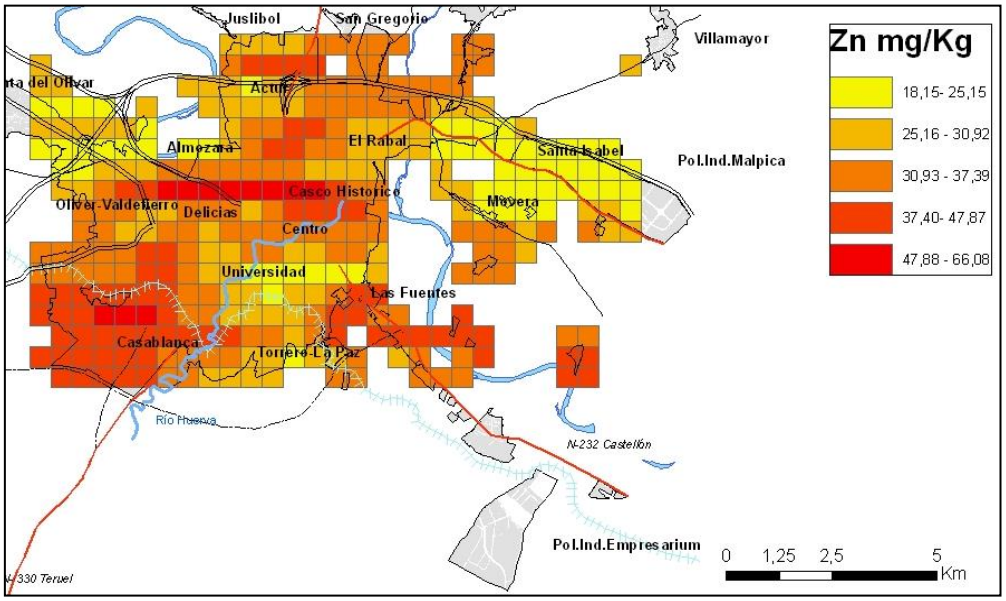

Figure 2. Maps of internal Cr, Ni, Pb, and Zn concentrations in *N. oleander* leaves.

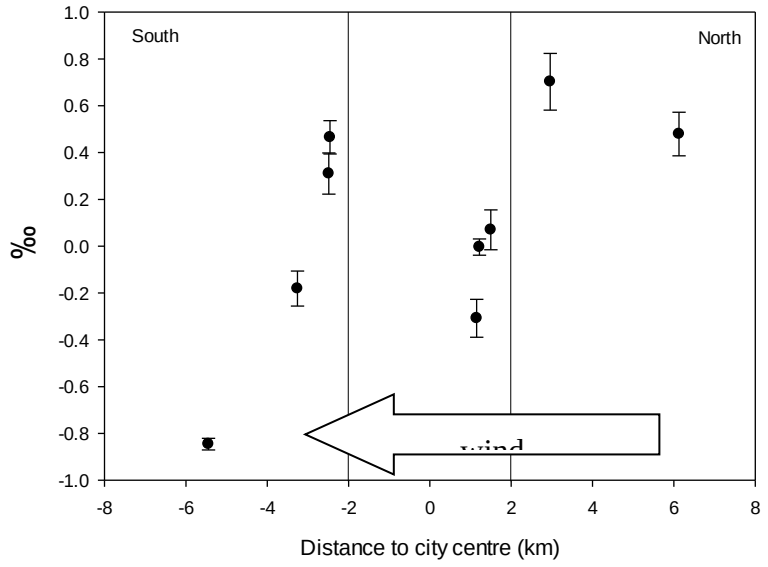

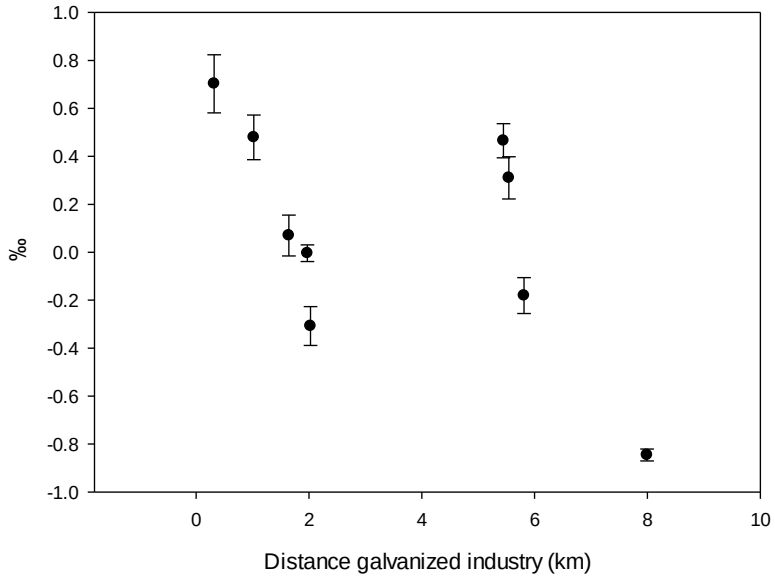

Figure 3. Upper. $\delta^{66}Zn_{Lyon}$ of *N. oleander* unwashed leaves vs the distance from the city centre (km) following a northwest-southeast section (the dominant wind direction). **Lower.** $\delta^{66}Zn_{Lyon}$ of *N. oleander* represented as a function of the distance to galvanizing industry (km). The $\delta^{66}Zn$ increases from south to north across the city centre (Fig. 3. upper); heavier isotopes are close to the main industrial region (located in the north) while the lighter ones are far from both the city centre and industries.

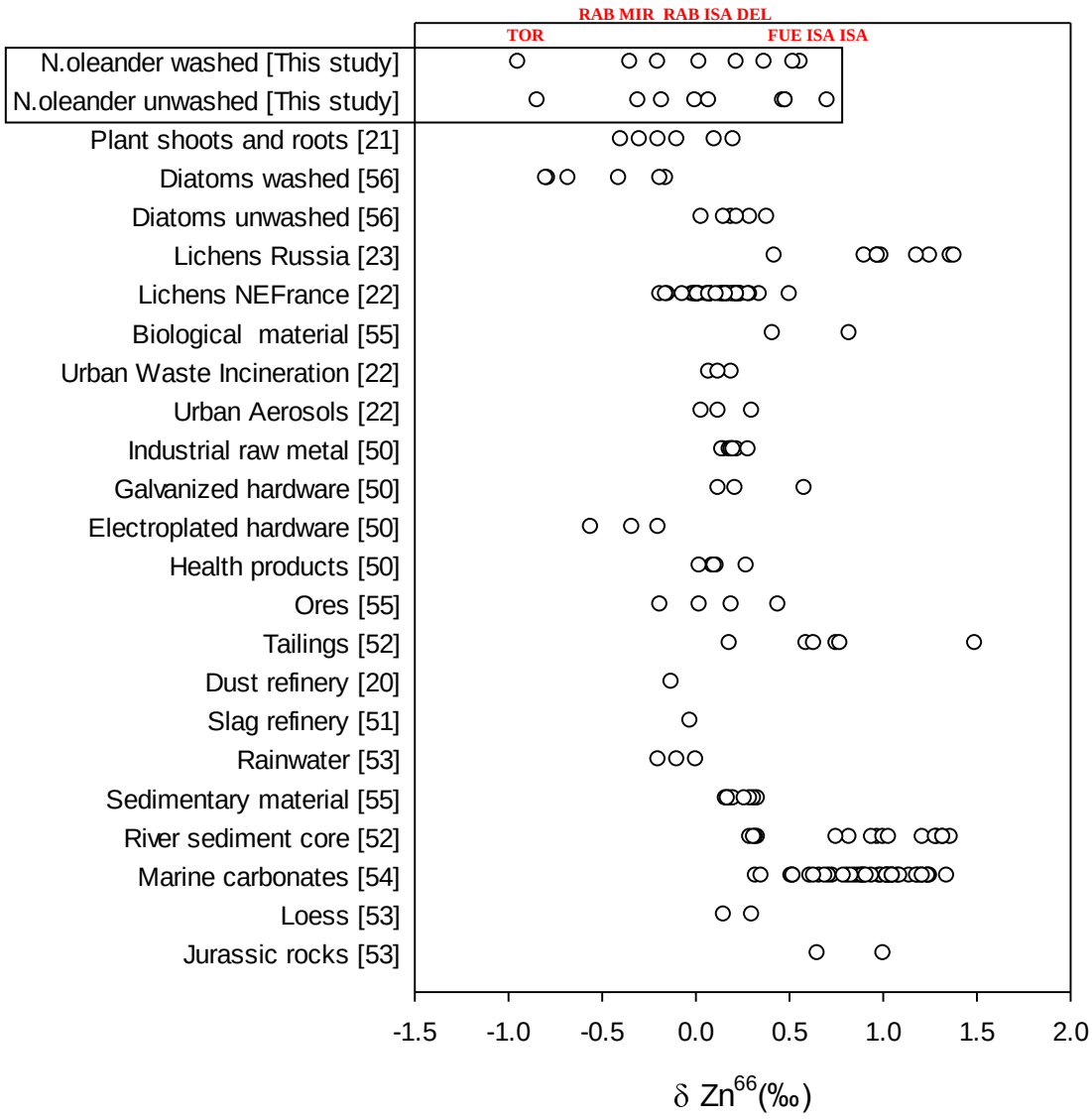

Figure 4. Zn isotopic composition ($\delta^{66}Zn_{Lyon}$) of different materials, including the *N. oleander* leaves of this study, which isotopic signatures range from values similar to those found in marine diatoms [56] or plants [21] to a mixture of industrial activities and long-range airborne transport of sediments and other materials as ores or rainfall. District codes (see Fig. 1) have been used to identify the samples.